Breast Cancer Research

The indole-3-carbinol cyclic tetrameric derivative CTet inhibits cell proliferation via overexpression of p21/CDKN1A in both estrogen receptor positive and triple negative breast cancer cell lines

Breast Cancer Research 2011, **13**:R33 doi:10.1186/bcr2855

Mauro De Santi (mauro.desanti@uniurb.it)
Luca Galluzzi (luca.galluzzi@uniurb.it)
Simone Lucarini (simone.lucarini@uniurb.it)
Maria Filomena Paoletti (maria.paoletti@uniurb.it)
Alessandra Fraternale (alessandra.fraternale@uniurb.it)
Andrea Duranti (andrea.duranti@uniurb.it)
Cinzia De Marco (Cinzia.DeMarco@istitutotumori.mi.it)
Mirco Fanelli (mirco.fanelli@uniurb.it)
Nadia Zaffaroni (Nadia.Zaffaroni@istitutotumori.mi.it)
Giorgio Brandi (giorgio.brandi@uniurb.it)
Mauro Magnani (mauro.magnani@uniurb.it)

ISSN 1465-5411

Article type Research article

Submission date 16 November 2010

Acceptance date 24 March 2011

Publication date 24 March 2011

Article URL http://breast-cancer-research.com/content/13/2/R33

The indole-3-carbinol cyclic tetrameric derivative CTet inhibits cell proliferation via overexpression of p21/CDKN1A in both estrogen receptor positive and triple negative breast cancer cell lines

Mauro De Santi [1], Luca Galluzzi [1], Simone Lucarini [2], Maria Filomena Paoletti [1], Alessandra Fraternale [1], Andrea Duranti [2], Cinzia De Marco [3], Mirco Fanelli [1], Nadia Zaffaroni [3], Giorgio Brandi [1*], Mauro Magnani [1]

[1] Department of Biomolecular Sciences, University of Urbino "*Carlo Bo*", Via Saffi 2, 61029 Urbino, Italy

[2] Department of Health and Drug Sciences, University of Urbino "*Carlo Bo*", Via Saffi 2, 61029 Urbino, Italy

[3] Department of Experimental Oncology and Molecular Medicine, Fondazione IRCCS Istituto Nazionale dei Tumori, Via G. Venezian 1, 20133 Milano, Italy

* Corresponding Author:

Giorgio Brandi

Email: giorgio.brandi@uniurb.it

Abstract

Introduction: Indole-3-carbinol (I3C), an autolysis product of glucosinolates present in cruciferous vegetables, and its dimeric derivative (3,3'-DIM), have been indicated as a promising agents in preventing the development and progression of breast cancer. We have recently shown that I3C cyclic tetrameric derivative CTet formulated in γ-cyclodextrin (γ-CD) efficiently inhibited cellular proliferation in breast cancer cell lines. This study aims to analyze the mechanisms involved in the *in vitro* inhibition of cell proliferation and to evaluate the *in vivo* antitumor activity of CTet in a xenograft study.

Methods: Estrogen receptor positive MCF-7 and triple negative MDA-MB-231 breast cancer cell lines were exposed to CTet to evaluate cell cycle perturbation (propidium iodide staining and cytofluorimetric acquisition), induction of autophagic morphological features (co-localization of LC3b autophagosome marker and LAMP2a lysosome marker by immunofluorescence) and changes in protein expression (immunoblot and microarray-based gene expression analyses). To test the *in vivo* efficacy of CTet, female athymic nude mice inoculated with MCF-7 cells were i.p. treated with 5 mg/kg/day of CTet for five days/week for two weeks and the tumor mass was externally monitored.

Results: CTet induced accumulation in G2/M phase without evidence of apoptotic response induction in both cell lines tested. In triple negative MDA-MB-231 the autophagic lysosomal activity was significantly up-regulated after exposure to 4 μM of CTet for 8 hours, while highest CTet concentration was necessary to observe autophagic features in MCF-7 cells. The inhibition of Akt activity and p53-independent p21/CDKN1A and GADD45A overexpression were identified as the main molecular events responsible for CTet activity in either MCF-7 and p53-mutant MDA-

MB-231 cells. *In vivo*, CTet administration was able to significantly inhibit the growth of MCF-7 xenotransplanted into nude mice, without adverse effect on body weight or on haematological parameters.

Conclusions: Our data support CTet formulated with γ-CD as a promising and injectable anticancer agent for both hormone-responsive and triple-negative breast tumors.

Introduction

Breast cancer is one of the most common malignancies in the industrialized countries, characterized by distinct classes of tumors that differently respond to targeted therapies such as Selective estrogen receptor modulators (SERMs) treatments (*e.g.* tamoxifen) in estrogen receptor-positive breast cancer or monoclonal antibodies (*e.g.* trastuzumab) in HER2/Neu-positive breast cancer. However, about 10-15% of breast cancers do not express estrogen (ER), progesterone (PR), and HER2/Neu receptors [1-2]. This subgroup, so-called triple-negative category, is associated with poor prognosis because resistant to therapy; its management includes the use of standard treatment such as platinum-based therapy, anthracycline and taxanes, nevertheless frequently associated with local and systemic relapse [2]. Therefore, a critical problem in the clinical strategies for the management of breast cancer is the development of molecules with effective activity in the treatments of hormone-responsive as well as triple-negative tumors. Several clinical trials assessing various therapeutic options, including the use of inhibitors of specific molecular targets such as Poly-(ADP-ribose)-polymerase (PARPs) or the mammalian target of rapamycin (mTOR), used as monotherapy or combined with traditional chemotherapy, are currently ongoing [1]. PI3K and downstream Akt/mTOR pathway represent potential targets for treatment of triple-negative breast cancer

because implicated in several cell responses such as regulation of cell growth, survival, and apoptosis [2,3].

Cruciferous vegetables consumption has been associated with lower cancer risk in several epidemiological and dietary studies [4-6]. The chemopreventive properties of these vegetables are attributed to anti-tumor activity of indole-3-carbinol (I3C) and its metabolic derivatives, that have shown a great potential both for prevention and treatment of cancer through numerous mechanisms such as induction of apoptosis and cell cycle arrest, antiestrogenic activity, gene expression modulation and prevention of carcinogen-DNA adduct formation [7,8]. It has also been reported that I3C and its major condensation product 3,3'DIM inactivate Akt signalling pathway in breast cancer cells [9-11]. Nevertheless, the development of I3C as a therapeutic agent is limited by several factors such as its easy conversion into many polymeric products *in vivo* [12]. These compounds have some common targets but have also been demonstrated to have distinct biological effects on breast cancer cells [13,14], and the relative high concentrations necessary to inhibit the expression of CDK6 and to induce cell cycle arrest in breast cancer (from 50 to 200 μM) [15,16].

Alternatively to I3C as chemotherapeutic agent for treatment of breast cancer, several I3C derivatives characterized by higher antiproliferative properties have been recently proposed [7, 17-19]. I3C cyclic tetrameric derivative CTet (5,6,11,12,17,18,23,24-octahydrocyclododeca[1,2-*b*:4,5-*b'*:7,8-*b''*:10,11-*b'''*]tetraindole) (Figure 1) is an anticancer molecule that has been shown to exert an interesting antiproliferative activity in both MCF-7 and MDA-MB-231 breast cancer cell lines [20]. Lucarini *et al.* have optimized a straightforward, reproducible and scalable CTet synthesis [21]. Moreover, to improve the bioavailability, they have optimized a formulation based on γ-CD aqueous solution that results about 10-fold more active respect to the first preparation [20].

In this study we analyze the biological responses in terms of cell cycle perturbations and autophagy induction in both estrogen receptor-positive (MCF-7) and triple-negative (MDA-MB-231) breast cancer cell lines exposed to CTet obtained by a new synthetic procedure. We also characterize the molecular mechanisms leading to the inhibition of cell proliferation using microarray-based gene

expression analysis. We identified the overexpression of p21/CDKN1A as the strongest molecular event induced by CTet treatment; the inhibition of Akt activity, revealed in CTet-treated cells, could be responsible for p21/CDKN1A overexpression in MCF-7 and p53-mutant MDA-MB-231 cells. Finally, the toxicity and antitumoral efficacy of the γ-CD-formulated CTet, obtained in a preliminary xenograft study, are discussed.

Materials and methods

Chemistry

All reagents, purchased from Sigma-Aldrich or Carlo Erba with the exception of γ-CD (CAVAMAX® W8, Wacker) were in the highest quality commercially available. Solvents were RP grade. Melting point, HPLC/MS, ^{1}H-NMR, and ^{13}C-NMR were determined as in [21]. Purification of the crude material was carried out as in [21]. TLC analyses were performed as in [21].

Synthesis of CTet

To a solution of 3-[(1*H*-indol-2-yl)methyl]-1*H*-indole (2,3'-DIM) [22] (0.246 g, 1 mmol) and 37% aqueous formaldehyde (0.122 mL, 1.46 mmol) in methanol (10 mL), 96% sulphuric acid (0.063 mL) was added and the mixture was refluxed in the dark for 1 hour. After cooling, the purple mixture was concentrated *in vacuo* in the dark. Purification of the resulting deep-purple solid by two short, protected from light, and fast aluminum oxide column chromatographies (cyclohexane/EtOAc 8:2) gave a white solid consisting (HPLC/MS) in a 2:1 mixture of CTr (5,6,11,12,17,18-esahydrocyclonona[1,2-*b*:4,5-*b'*:7,8-*b''*]triindole) and CTet (yield: 45%, 0.117 g), which was recrystallized from acetone (12 mL). CTet was obtained as a pure white solid. CTet yield: 16% (0.041 g). Mp, ^{1}H-NMR, and ^{13}C-NMR are according to the literature [21].

Cell culture

The human breast carcinoma ER+ (MCF-7, BT-474) and triple-negative (MDA-MB-231, BT-20) cell lines were cultured in DMEM (Dulbecco's Modified Eagle's Medium) supplemented with 10% FCS (Fetal Calf Serum), 2 mM L-glutamine, 10 g/L NEAA (Non-Essential Amino Acid), 50 mg/L streptomycin, 1000 U/L penicillin, with 10 mg/L insulin (in MCF-7 cells), at 37°C in humidified incubator with 5% CO_2. For the *in vivo* experiments MCF-7 cells were cultured in complete medium supplemented with 1 nM β-estradiol 17-cypionate for two weeks. All cell culture materials were purchased from Sigma-Aldrich (St. Louis, MO).

CTet was formulated with aqueous γ-CD solution as reported by Lucarini *et al.* [21]. In all experiments, 10 µl of the concentrated agent was added to 1 ml of cell culture medium (vehicle control, 10 µl of aqueous solution of γ-CD).

Cell treatments

Cell proliferation was evaluated using [^{3}H]thymidine (Sigma) incorporation assay. Cells were seeded at a density of 30,000/well in 24-well tissue culture plates and allowed to attach overnight. Duplicate samples were treated for 72 h with increasing concentrations of CTet (from 0.5 to 8.0 µM). During the last 5 hours of treatment, cells were pulsed with 3 µCi/well of [^{3}H]thymidine (25 Ci/mmol) and processed as reported by Brandi *et al.* [20]. Briefly, cells were washed three times with ice-cold trichloroacetic acid (10% w/v) and lysed with 300 µl of 0.3 N NaOH. Aliquots (150 µl) of lysate were transferred into scintillation vials and processed for liquid scintillation counting. The results are expressed as the percentage of average cpm value in drug-treated samples compared with control samples.

In a set of experiments one batch of CTet was suspended in pure EtOH and aliquoted to evaluate the activity in different storing conditions. One aliquot was diluted in γ-CD and immediately tested in the antiproliferative assay. Three aliquots were stored at the following conditions: 1) room temperature (R.T.) exposed to light, 2) R.T. protected to light, 3) +4°C protected to light. Other

three aliquots were diluted 1:10 in aqueous solution of γ-CD and stored at the same conditions. The antiproliferative activity was evaluated in MCF-7 cells using [^{3}H]thymidine incorporation assay at different time points up to one year.

For the gene expression, immunoblot and cell cycle analyses, breast cancer cells were plated in 6-wells culture plates at density of 150,000 cells/well and cultured overnight. Cellular treatments were conducted at increasing concentration of CTet, or vehicle control, for 24 and 48 hours. Cell survival was then evaluated by trypan blue dye exclusion assay and, after washing in phosphate buffered saline (PBS), the cells were pelletted by centrifugation and immediately used for cell cycle analysis or stored at -20°C (for successive immunoblot blot or gene expression analyses). Cellular pellets prepared for gene expression analysis were stored with 300 µl of RNA-later (Sigma).

HPLC analyses

Quantitative determinations of CTet were performed using a HPLC-UV method (JASCO Model PU-980). The compound was separated at RT on a Tracer Excel 120 ODSA 5 µm 15×0.46 column protected by a guard column (Pelliguard LC-18, 20 mm×4.6 mm i.d., 40 µm); columns were from Teknokroma (Barcelona, Spain). CTet was quantified by UV detection at 280 nm. The volume injected was 50 µl. The mobile phase consisted of two eluents: 100% H_2O (buffer A); 100% acetonitrile (buffer B) and CTet was eluted using a flow rate of 1.0 ml/min and the following steady gradient program: 100% buffer A for 3 min, taken to 40% buffer B over the next 12 min, rising to 80% buffer B from 15 min to 25 min; this condition was hold for 5 min; the gradient was returned to 100% buffer A in 5 min.

Cell cycle analysis

Cell cycle was analysed using the propidium iodide staining procedure as previously reported [23]. Briefly, cells were fixed in ice-cold 70% ethanol solution (16 hours at +4°C) and stained in

propidium iodide solution (0.1% sodium citrate, 0.1% Triton X-100, 250 μg/ml RNase A, 50 μg/ml propidium iodide). Cytofluorimetric acquisitions and sample analysis were performed by Partec PAS flow cytometer (Partec, Münster, Germany) and FlowJo 8.6.3 software (Tree Star, Inc., Ashland, OR, USA), respectively.

Autophagy detection by immunofluorescence analyses

MCF-7 and MDA-MB-231 cells were grown in complete medium on glass coverslips in 6-well plates. After 24 hours attachment, cells were treated with CTet for 4, 8, 12 and 24 hours. At the end of each treatment, cells were fixed with PBS containing 4% formaldehyde for 15 min and permeabilized with methanol/acetone solution for 15 min at R.T. To assess the colocalization of LC3b with the lysosome marker LAMP2a, cells were incubated with a mixture containing the anti-LC3b (Sigma) and LAMP2a (Abcam, Cambridge, UK) primary antibodies, washed and then probed with goat anti-rabbit AlexaFluor498 and goat anti-mouse AlexaFluor594 secondary antibodies. Nuclei were counterstained with 0.1 μg/ml DAPI. Images were acquired by a Nikon Eclipse E600 microscope using ACT-1 software and processed with an Adobe Photoshop Image Reader 7.0.

Gene expression analysis

RNA extraction and microarray analysis

Whole genome microarray analysis was performed using CodeLink Expression Bioarray System (GE Healthcare, Piscataway, NJ) either on MCF-7 or MDA-MB-231 cells treated with 6 μM and 12 μM CTet for 24 h. Total RNA was purified from treated and control cells using the RNeasy plus kit (Qiagen, Hilden, Germany). The RNA was quantified spectrophotometrically using Nanodrop ND-1000 (Thermo Fisher Scientific); moreover, RNA integrity was evaluated using the Experion automated gel electrophoresis system (Bio-Rad, Richmond, CA). Biotin-labeled cRNA was

synthesized using the CodeLink iExpress Assay reagent kit (GE Healthcare), following the manufacturer's protocols. Biotin-labeled cRNA obtained from each control or treated biological sample was fragmented and hybridized against three independent arrays (10 μg each) at 37°C for 22 hours (*i.e.*, three replicates for each biological sample). After hybridization, the arrays were washed, stained with Cy5-streptavidin and scanned using a ScanArray GX scanner (Perkin Elmer, Norwalk, CT), with a resolution of 5 μm.

The image files generated by the scanner were processed using the Codelink Expression Analysis software (GE Healthcare). Normalized data from the Codelink software package were analyzed with GeneSifter software (Geospiza Inc., Seattle, WA) [24] for statistical validation and data mining. This comprehensive software also generated gene ontology (GO) and z-score reports. The z-score is useful for ranking GO terms by their relative amounts of gene expression changes. Positive z-scores indicate GO terms with a number of differentially expressed genes higher than expected by chance, while negative z scores indicate GO terms with a number of differentially expressed genes lower than expected by chance [25]. The whole data set obtained from the two experiments on MCF-7 and MDA-MB-231 cells, both including technical replicates for each control and treated sample, were subjected to analysis of variance (ANOVA) and 5% false discovery rate calculation [26]. The cut-off parameters for differential gene expression were p =0.01 and fold change threshold =2. Microarray data are available in MIAME compliant ArrayExpress database [27] (accession number [E-MEXP-2989]).

Quantitative real-time PCR

Real-time (RT) PCR was used to validate the gene expression profiles observed in the CodeLink microarray experiments. cDNA was synthesized from the same total RNA used for microarray experiments, using SuperScript First Strand Synthesis System for RT-PCR (Invitrogen, Carlsbad, CA) with oligo-dT priming. Primers for amplification of p27/CDKN1B were p27F 5'-GCAGGAATAAGGAAGCGACCT-3' and p27R 5'-TCCACAGAACCGGCATTTG-3', while

primers for the amplification of p21/CDKN1A and GADD45A, together with primers for the amplification of housekeeping genes ACTB (actin-β) and GAPDH (Glyceraldehyde-3-phosphate dehydrogenase), have been described elsewhere [23]. All primer pairs spanned an intron to avoid amplification of contaminating genomic DNA. RT-PCR reactions were performed in triplicate in a final volume of 25 µl using SYBR green PCR master mix (Applied Biosystems, Foster City, CA) with 200 nM primers, in a RotorGene 6000 instrument (Corbett life science, Sydney, Australia). The cycling protocol was: 95°C 10 min followed by 40 cycles at 95°C for 10 s and 60°C for 45 s. At the end of each run, a melting curve analysis from 55°C to 90°C was performed to ensure the absence of primer dimers or non-specific products. Fold changes were calculated using the comparative quantification application of the RotorGene 6000 software. Real-time PCR-based gene expression analysis was also repeated on two new sets of biological samples, both from MCF-7 and MDA-MB-231 cells.

Immunoblot analysis

Untreated and CTet-treated cells were lysed for 20 min on ice with 20 mM HEPES (pH 7.9), 25% glycerol, 0.42 M NaCl, 0.2 mM EDTA, 1.5 mM $MgCl_2$, 0.5% Nonidet P-40, 1x Complete protease inhibitor cocktail (Roche Diagnostics Ltd, Mannheim, Germany). Cell lysate was frozen and thawed twice and clarified by centrifugation at 12,000 rpm for 10 min at 4°C. Subcellular fraction was obtained as follows: cells were lysed for 10 min on ice with 10 mM HEPES ph 7.9, 1.5 mM $MgCl_2$, 10 mM KCl, 1 mM EDTA, 1 mM Na_3VO_4, 1 mM NaF, 1 mM DTT, 0.1 % Nonidet P-40, 1x Complete protease inhibitor cocktail. Samples were then centrifuged at 12,000 rpm for 10 min at 4°C to obtain the cytosolic fraction (supernatant); the pellet was resuspended in 20 mM HEPES (pH 7.9), 25% glycerol, 0.42 M NaCl, 0.2 mM EDTA, 1.5 mM $MgCl_2$, 1 mM Na_3VO_4, 1 mM NaF, 1 mM DTT, 1x Complete protease inhibitor cocktail, incubated 20 min on ice and centrifuged at 12,000 rpm for 10 min at 4°C to obtain nuclear fraction (supernatant).

Protein extracted were fractionated on 12% (p27 and p21) and 7.5% (Akt, phospho-Akt and FOXO3a) SDS-PAGE, and then electrically transferred to Trans-Blot transfer medium (0.2 µm) nitrocellulose membrane (Bio-Rad, Hercules, CA). Blots were incubated with anti-p27 (1:500), anti-p21 (1:200) antibodies purchased from Santa Cruz Biotechnology (Santa Cruz, CA), anti-Akt and anti-phospho-Akt(Ser473) antibodies purchased from Cell Signaling Technology (Beverly, MA) and anti-FKHRL1/FOXO3a (1:1000) antibody purchased from Upstate (Lake Placid, NY) overnight at 4°C, and then 1 hour at R.T. with peroxidase-conjugated secondary antibody. Blots were treated with enhanced chemiluminescence reagents, and all of the proteins were detected and quantitated by ChemiDoc System (Bio-Rad). Equal protein loading was confirmed by the level of actin protein present in the membrane tested with anti-actin antibody 1:500 (Sigma, St. Louis, MO).

In vivo tumor growth inhibition

Housing and treatment of mice were in compliance with the Guide for the Care and Use of Laboratory Animals by Ministero della Sanità D.L. 116, 1992 and approved by the university committee for animal experiments.

Female athymic Crl:CD-1-nu/nuBR nude mice, 4 weeks of age (Charles River Laboratories, Milan, Italy) were housed under pathogen-free conditions. They were acclimated for 1 week.

β-estradiol 17-cypionate (Sigma) was intramuscularly injected at 3 mg/Kg one week before MCF-7 cells were transplanted into the animal and then once weekly for the duration of the experiment to support the growth of the estrogen-dependent MCF-7 tumors. The cells were inoculated subcutaneously at $1.1x10^6$ cells/inoculum on one flank in a final volume of 200 µl containing 100 µl of Matrigel (BD Biosciences, US) and 100 µl of cells suspended in 0.9% NaCl.

Twenty days after the cell inoculation, the mice received the CTet intraperitoneally (i.p.) at the concentration of 5 mg/Kg/day, for 5 days/week for a total of two weeks. The mice in the control (placebo) group received the same volume of the vehicle as the CTet-treated mice. At least four animals were studied for each experimental group. Each xenograft was monitored by externally

measuring tumors in two dimensions using a calliper. Tumor volume (mm^3) was calculated as a^2 x b x 0.5, where a is the length and b is the width of the tumors.

Statistical analyses

Data are expressed as mean ± SEM of at least three separate experiments. The IC_{50}s of antiproliferative activity were calculated by non-linear regression using the equation $y = 100 - Top \cdot x^{(HillSlope)}/(IC_{50}^{(HillSlope)} + x^{(HillSlope)})$ (Prism5, GraphPad Software Inc., La Jolla, CA). Statistical analysis were performed using Mann-Whitney test or one-way ANOVA followed by Tukey post-hoc test as appropriate (Prism5).

Results

Synthesis of CTet

The protocol herein reported to obtain CTet was optimized in terms of reagents, temperature and time. The developed method proved to be reproducible with regard to CTet/CTr ratio and yield (Additional data file 1. CTr formation).

Antiproliferative activity of CTet

It has been previously reported that CTet formulated with γ-CD is able to inhibit proliferation of both MCF-7 and MDA-MB-231 breast cancer cell lines [21]. In this study we confirm the dose-dependent activity of CTet in both MCF-7 (IC_{50} = 1.32 ± 0.03 μM) and MDA-MB-231 (IC_{50} = 1.00 ± 0.01 μM). In addition, we investigated the drug effect on DNA synthesis in other two breast cancer cell lines, BT474 (ER+) and BT-20 (triple-negative) (Figure 2). The IC_{50} values obtained in the two cell lines were 2.64 ± 0.28 and 6.69 ± 0.37 μM, respectively.

Analysis of cell cycle perturbations

Cell cycle analysis was carried out in MCF-7 and MDA-MB-231 to evaluate the effect of CTet in cell cycle progression. Cells were treated with CTet for 24 and 48 hours at the final concentrations of 4.0 μM and 8.0 μM and then stained with propidium iodide for flow cytometric analyses. Results showed that CTet induced G2/M accumulation in both MCF-7 and MDA-MB-231cells (Figure 3). After 48 hours of treatment, the cellular population in G2/M phase significantly increased from 19.7 ± 0.9 to 25.4 ± 0.9 % in MCF-7 and from 19.5 ± 1.5 to 26.1 ± 0.6 % in MDA-MB-231 ($p<0.05$).

CTet-treated MDA-MB-231 cells show morphological features of autophagy

Although the exposure of breast cancer cells to CTet failed to induce apoptosis, specific morphological features of autophagy were detectable in drug-treated MDA-MB-213 cells. In particular, in cells exposed for different time points to 8.0 μM CTet, the occurrence of autophagy was assessed by immunofluorescence analysis of LC3b protein. The LC3b protein is recruited to the autophagosome membrane during autophagy process and, consequently, changes in the intracellular localization of LC3b provide a reliable molecular marker for the detection of autophagy. A significant increase in the percentage of MDA-MB-231 cells with a characteristic punctate pattern of LC3b expression was appreciable following exposure to CTet (Figure 4a). Fusion between autophagosomes and lysosomes also represents an important regulatory step of autophagy pathway and can be monitored by co-localization of LC3b and lysosome markers LAMP1 or LAMP2a. In MDA-MB-231 cells, autophagic vescicles were found to co-localize with lysosome after exposure to CTet, as demonstrated by the overlapping of LC3b and LAMP2a signals in combined immunofluorescence experiments (Figure 4b; Additional data file 2, Fig. 1S). Taken together these results indicate that autophagic lysosomal activity is significantly up-regulated in MDA-MB-231 as a consequence of CTet exposure. Autophagy features have been transiently observed also in MCF-7 cells following exposure to the highest CTet concentration (data not shown).

Changes of gene expression profile induced by CTet in MCF-7 and MDA-MB-231cell lines.

The molecular mechanisms involved in CTet-response in MCF-7 and MDA-MB-231 cells lines were investigated using microarray technology. Both cell lines were treated with 6.0 μM and 12.0 μM CTet for 24 hours before cell harvesting. This early time point was chosen with the aim to observe the changes in gene expression before they have effect on cell metabolism. Since the antiproliferative activity and biological responses of CTet were similar among cell lines and independent from the hormonal receptor status, the genes sharing a common expression pattern in both MCF-7 and MDA-MB-231 cell lines, either in 6.0 μM and 12.0 μM CTet treatment conditions, were selected using GeneSifter software.

First, using a differential expression cutoff =2 (ANOVA, Benjamini–Hochberg false discovery rate correction, $p<0.01$), a total of 960 genes differentially expressed in at least one treatment in MCF-7 and/or MDA-MB-231 cells were identified. Then, a further analysis of the expression pattern in this subset of genes (Pearson uncentered correlation coefficient = 0.98) revealed that 116 genes were up-regulated, (search pattern: control =1; 6.0 μM >1; 12.0 μM >2) and 177 genes were down-regulated (search pattern: control =1; 6.0 μM <1; 12.0 μM <0.5) in both cell lines (Additional data files 3 and 4, Tables 1S and 2S, respectively). To explore the biological significance of the transcriptome response shared by both cell lines, z-score reports containing the most significant GO terms were generated from the commonly up-regulated (Table 1) and down-regulated genes (Table 2). Criteria for selection were: GO terms containing ≥20 genes; number of genes differentially expressed within the assigned ontology ≥ 3; z-score ≥ 4 or ≤ -4. The ontology list was then pruned by hand for related GO terms to remove any over-represented branches of the GO hierarchy. When both a parent and a child term were present in the list, the parent term was removed if its presence was due entirely to genes meeting the criterion for the child term.

Concerning the up-regulated genes, the main terms in the biological process category included "response to stimulus" (stress, chemical stimulus, extracellular stimulus, etc.), "apoptosis", "protein

folding" and "autophagy". The cellular components were linked to "autophagic vacuole" and "integral to membrane", this latter having a number of differentially expressed genes lower than expected by chance (negative z-score; see methods). In the molecular function category, transcripts were linked to "heat shock protein binding", "unfolded protein binding" and "antioxidant activity" (Table 1).

With respect to down-regulated genes, the biological process category included "cell cycle" and "DNA metabolic process", while the cellular components were linked to "chromosomal part". Finally, the molecular functions category included "transmembrane receptor protein tyrosine kinase activity", "DNA helicase activity" and "insulin-like growth factor binding" (Table 2).

To further verify the microarray transcription profile results, selected genes were analyzed by quantitative RT-PCR. For these analyses, three genes associated with cell cycle arrest were selected: p27 (already identified by using CTet previously prepared [20]), GADD45A and p21/CDKN1A (identified as γ-CD-formulated CTet-induced genes in the microarray experiments). GAPDH was used as housekeeping gene. Actin-β was used as alternative housekeeping gene to confirm the results obtained with GAPDH, in a subset of samples (not shown). The results (Figure 5) were almost superimposable with the microarray experiments, although a greater sensitivity of RT-PCR compared to microarray analysis was revealed. p27/CDKN1B gene expression appeared unchanged, while p21/CDKN1A showed up-regulation in all conditions tested in both cell lines. Moreover, a significative up-regulation of GADD45A gene was observed in both MCF-7 and MDA-MB-231 cell lines, despite the microarray experiment did not show any significant up-regulation in the latter cell line. The quantitative real-time PCR analysis has been also performed on two new sets of biological samples, either from MCF-7 or MDA-MB-231 cells, confirming the up-regulation of p21/CDKN1A and GADD45A. The average data obtained from three biological samples are shown in Additional data file 5, Fig. 2S.

Immunoblot analysis

The significant upregulation of p21/CDKN1A CDKs inhibitor gene, monitored by microarray studies, was further investigated at the protein level by immunoblot analysis. The results showed that p21/CDKN1A was overexpressed in both MCF-7 and MDA-MB-231 cell lines after 24 hours of treatment (> 7-fold to actin), and in MCF-7 cells also after 48 hours of treatment (> 9-fold to actin), (Figure 6). Differently from the previous results [20], CTet formulated did not induce $p27^{kip1}$ overexpression in MCF- 7 and MDA-MB-231 cells.

Further investigations were therefore directed to establish the involvement of FOXO3a transcription factor localization and Akt activity, both involved in p21/CDKN1A expression [28,29]. To evaluate the role of PI3K/Akt pathway in p21/CDKN1A expression in CTet-treated breast cancer cell lines, Akt activity was detected using a specific anti phospo-Akt antibody, the phosphorylated form of Akt protein. The results showed that in both MCF-7 and MDA-MB-231 phospho-Akt decreases after 48 hours of treatment (about 0.8-fold and 0.6-fold to total-Akt in MCF-7 and MDA-MB-231 respectively), while the decrement of the cytosolic fraction of phospho-Akt was observed after 24 hours of treatment (about 0.6-fold and 0.4-fold to total-Akt in MCF-7 and MDA-MB-231 respectively) (Figure 6). Akt can inactivate FOXO3a via phosphorylation and subsequent translocation to cytosol but, in CTet-treated cell, there was no evidence of variation in FOXO3a localization suggesting that this transcription factor was not involved in the overexpression of p21/CDKN1A.

Effect of CTet on xenograft tumor growth in athymic nude mice

Toxicity studies aimed at establishing lethal dose (LD50), showed that CTet in the concentration range 0.5-15 mg/Kg did not cause any toxic effect (data not shown).

To evaluate the potential therapeutic efficacy of systemic administration of CTet, a preliminary experiment was performed in human breast cancer xenograft-bearing nude mice. The MCF-7 cells were inoculated subcutaneously on one flank of nude mice as described under “materials and methods” section. Twenty days after cell inoculation, i.p. treatment with the CTet at the dose of 5

mg/Kg/day, five treatments a week, was started and lasted for two weeks. The results showed that the treatment blocked the increase of tumor mass, which significantly increased in the animals either not treated or receiving the vehicle (Figure 7). After two weeks of treatment, both mice groups receiving CTet or the vehicle, did not show either alteration in body weight or in the haematological parameters respect to the untreated mice (data not shown).

CTet activity in different storing conditions

CTet activity in different storing conditions was evaluated up to one year. Aliquots of CTet were stored at different conditions of temperature and light exposition (Additional data file 6, Table 3S) and the activity was then evaluated in MCF-7 at different time points (4, 8, 12, 20 weeks and after one year). The results showed that the antiproliferative activity, expressed as IC_{50}, remains nearly unchanged up to one year (Additional data file 6, Table 3S). Chemical stability of the molecule was assessed by HPLC after one year of storage. The chromatographic profile showed that in all light protected conditions more than 95% of the CTet maintained its chromatographic behaviour confirming the biological data, while in not light protected conditions a loss of the molecular integrity (~15%) was detected (data not shown).

Discussion

In the last decades the mortality rates of breast cancer have decreased [30] as a result of implementation of screening [31], improvements in the local management of early breast cancer [32], and the introduction of adjuvant systemic treatments [33]. However, breast cancer is the leading cause of cancer-related death for women in Europe and US [34,35]. The treatment of subgroup of breast tumors resistant to targeted therapies - named triple-negative tumors because lack of estrogen, progesterone, and HER2/Neu receptors - is a problem that still remains unsolved [1-2].

Derivatives of indole-3-carbinole (I3C) with a good antiproliferative activity independently of hormonal receptor status have been widely studied in the last years [7,8, 17-19, 36].

Among these molecules it was shown the potential of the I3C cyclic tetrameric derivative CTet in the inhibition of breast cancer cell proliferation [20]. However, further analysis revealed that the synthetic method previously reported did not give a pure compound due to the presence of other oligomeric derivatives of I3C.

Recently, Lucarini *et al.* [21] have proposed a straightforward synthesis of CTet but this method, as well as the others reported in the literature [20,37,38], are not sufficiently advantageous. In this paper, we describe a new synthesis, involving 2,3'-DIM homo-coupling in the presence of formaldehyde in acidic medium. This synthetic procedure gave an acceptable CTet yield, higher than those already reported [20,21,37,38].

The antiproliferative activity of CTet formulated with γ-CD, firstly evaluated in MCF-7 and MDA-MB-231 [21], was confirmed in this study in two additional breast cancer cell lines (BT-474 and BT-20) showing that CTet is able to inhibit cell proliferation about ten-fold more than the first formulation in all cell lines tested.

The cell cycle and molecular analyses in MCF-7 and MDA-MB-231 cells treated with formulated CTet did not show the induction of G1 cell cycle arrest and/or the overexpression of CDKs p27 inhibitor as described previously [20]. In fact, CTet inhibited cell proliferation by activating mechanisms resulting in increased amount of viable cells in G2/M phase of cell cycle .

Autophagy is a multi-step process in which cellular proteins and organelles are sequestered, delivered to lysosomes, and digested by lysosomal hydrolases. This process culminates when the nascent autophagosome fuses with the endosomal/lysosomal system to create a fully functional degradative compartment, the autolysosome. By a combined immunofluorescence approach, we were able to detect such a fusion in CTet-treated MDA-MB-231 cells, as the co-localization of the autophagosome marker LC3b and the lysosomal marker LAMP2a [39]. Whether treatment-induced autophagy in these cells represents a survival mechanism or initiates a nonapoptotic cell death still

remains uncertain [40]. However, the evidence of a significant drug-induced antiproliferative effect in the absence of a clear activation of apoptotic pathways, as observed in gene expression analysis (see below), would suggest the possibility that MDA-MB-231 cells undergo autophagic cell death.
From gene expression analysis, a reliable list of genes up- or down-regulated in response to CTet treatment was obtained. Interestingly, several genes involved in suppression of cell proliferation resulted up-regulated (*e.g.* IL6, IL8, p21/CDKN1A, HBP1) while other genes involved in cell cycle progression were down-regulated (*e.g.* CDK2, CCNE2, E2F2, MCM3, PKMYT1), recapitulating the cell cycle profile alterations observed.
The gene expression analysis revealed also the cellular response to the stress/stimulus induced by the drug treatment, through the up-regulation of genes involved in oxidative stress response (*e.g.* HMOX1, TXNRD1, SOD2), xenobiotic metabolism, (*e.g.* CYP1B1, AKR1C1, AHR), response to unfolded proteins (*e.g.* DNAJB1, DNAJB4, DNAJB9, HSPA1A) and inflammatory response (*e.g.* IL6, CEBPB, CCL5, PTGS2, CFB). Moreover, the up-regulation of either pro-apoptotic (*e.g.* BBC3, DEDD2, PMAIP1) or anti-apoptotic genes (*e.g.* BAG3, BEX2) do not evidence any apoptosis induction. In addition, microarray results supported (from a molecular point of view) the autophagy process observed in both cell lines. In fact, the autophagy-related genes WIPI1 (ATG18), GABARAPL1 (ATG8), MAP1LC3B (LC3B) and SQSTM1 were found up-regulated.
Moreover, real-time PCR results, besides confirming the up-regulation of p21/CDKN1A, showed a significant up-regulation of GADD45A gene also in MDA-MB-231 cells.
Altogether, our results suggest that the genes responsible for arrest of cell proliferation could be the p21/CDKN1A and GADD45A. The p21 protein is a universal inhibitor of cyclin-dependent kinases (CDKs) family [41] and is able to block cell cycle progression in either G1/S and G2/M phases [41-44]. GADD45A interacts with Cdc2 and inhibits its kinase activity, playing an important role in regulation of the G2/M cell cycle checkpoint [45,46]. This finding suggests that CTet treatments inhibit cell cycle progression in breast cancer cells by acting on both G1/S and G2/M cell cycle checkpoints.

The up-regulation of p21/CDKN1A and GADD45A has to be considered not dependent by p53 induction since p53 gene is mutated in MDA-MB-231 cells [47,48]. Moreover, a search for the important transcription factor binding sites enriched in the selected 116 commonly up-regulated genes (Table 4S) using Distinct Regulatory Elements of co-regulated genes (DiRE) algorithm [49,50], did not show the presence of p53 among the top 50 transcription factors identified (not shown).

The immunoblot analysis also revealed the inhibition of Akt activity in both cell lines tested. The protein kinase components of protein kinase B (Akt) pathway represents one of the potential targets for treatment of triple negative tumors [2]. In fact, PI3K and downstream AKT/protein kinase B family members have been implicated in several cell responses, including the protection of cells from apoptosis, the promotion of cell proliferation, and different metabolic responses [3], and may also be implicated in both p53-dependent and p53-independent expression of p21/CDKN1A [28] and GADD45A [51]. The inhibition of Akt activity could then play a central role in the antitumoral properties of CTet, as well as I3C and 3,3'DIM [9-11], and could explain, at least in part, the induction of p53-independent p21/CDKN1A and GADD45A overexpression in the p53 mutant MDA-MB-231 cell line.

The mechanisms by which CTet-induced overexpression of p21/CDKN1A and GADD45A resulting in the inhibition of cell proliferation and autophagy will be further investigated to establish eventual involvement of upstream PI3K/AKT and/or other molecular pathways.

The *in vivo* biological activity of the γ-CD-formulated CTet was promising since the administration was effective in blocking the increase of tumor mass in xenograft study. Moreover, neither CTet formulation nor γ-CD aqueous solution alone showed toxicity.

CTet stored in the dark is a very stable molecule. Indeed, more than 98% of CTet formulated in γ-CD aqueous solution and stored at room temperature protected from light, retained its stability and biological activity up to one year ($IC_{50} < 1$ μM) in MCF-7 cells. On the whole, the results obtained

with γ-CD formulated CTet is very important because the utilization of DMSO as vehicle is not needed [17,20,36].

Conclusions

In conclusion, our results showed that CTet is able to induce G2/M cell accumulation and autophagic response in both hormone-responsive and triple-negative breast cancer cells. The overexpression of p21/CDKN1A could be the main molecular event responsible for the inhibition of cell proliferation, together with the inhibition of Akt activity and the overexpression of GADD45A and the autophagy-related genes. Results from the *in vivo* study also showed that CTet formulated with γ-CD is a promising and injectable anticancer agent, which deserves additional studies to support the data here reported.

Abbreviations

ER: estrogen receptor; PR: progesterone receptor; I3C: indol-3-carbinol; CTet: indole-3-carbinol cyclic tetrameric derivative; CTr: indole-3-carbinol cyclic trimeric derivative; γ-CD: γ-cyclodextrin; R.T.: room temperature; DMSO: dimethyl sulfoxide; GO: gene ontology; IC_{50}: half inhibitory concentration; p21/CDKN1A: cyclin-dependent kinase inhibitor 1A; $p27^{Kip1}$: cyclin-dependent kinase inhibitor 1B; GADD45A: growth arrest and DNA-damage-inducible protein alpha; LC3b: microtubule-associated protein 1 light chain 3; LAMP2a: lysosome-associated membrane protein type 2a; SEM: standard error medium.

Competing interests

MM and GB are listed as inventors on US Patent 7,645,788, “Tetramerous derivative of indole-3-carbinol with anti-carcinogenic activity and method of synthesis of said derivative”, held by the University of Urbino. The remaining authors declare that they have no competing interests.

Authors' contributions

MM and GB coordinated the studies and helped to design the experiments. MDS performed cell culture experiments and immunoblot analyses and drafted the manuscript. LG carried out the gene expression analyses. SL and AD performed and optimized the synthesis of CTet. MFP and AF carried out the xenograft experiments and HPLC analyses. MF performed the cytofluorimetric analyses. CDM and NZ carried out immunofluorescence analyses for the autophagy detection. All authors helped to draft the manuscript. All Authors read and approved the final manuscript.

Acknowledgements

This work was supported in part by the Italian Association for Cancer Research (AIRC).

References

1. Chacón RD, Costanzo MV: **Triple-negative breast cancer.** *Breast Cancer Res* 2010, **12 Suppl 2:**S3.
2. Cleator S, Heller W, Coombes RC: **Triple-negative breast cancer: therapeutic options.** *Lancet Oncol* 2007, **8:**235-244.
3. Coffer PJ, Jin J, Woodgett JR: **Protein kinase B (c-Akt): a multifunctional mediator of phosphatidylinositol 3-kinase activation.** *Biochem J* 1998, **335:**1-13.
4. Higdon JV, Delage B, Williams DE, Dashwood RH: **Cruciferous vegetables and human cancer risk: epidemiologic evidence and mechanistic basis.** *Pharmacol Res* 2007, **55:**224-236.
5. Minich DM, Bland JS: **A review of the clinical efficacy and safety of cruciferous vegetable phytochemicals.** *Nutr Rev* 2007, **65:**259-267.

6. Verhoeven DT, Goldbohm RA, van Poppel G, Verhagen H, van den Brandt PA: **Epidemiological studies on brassica vegetables and cancer risk.** *Cancer Epidemiol Biomarkers Prev* 1996, **5:**733-748.

7. Weng JR, Tsai CH, Kulp SK, Chen CS: **Indole-3-carbinol as a chemopreventive and anti-cancer agent.** *Cancer Lett* 2008, **262:**153-163.

8. Aggarwal BB, Ichikawa H: **Molecular targets and anticancer potential of indole-3-carbinol and its derivatives.** *Cell Cycle* 2005, **4:**1201-1215.

9. Howells LM, Gallacher-Horley B, Houghton CE, Manson MM, Hudson EA: **Indole-3-carbinol inhibits protein kinase B/Akt and induces apoptosis in the human breast tumor cell line MDA MB468 but not in the nontumorigenic HBL100 line.** *Mol Cancer Ther* 2002, **1:**1161-1172.

10. Rahman KM, Li Y, Sarkar FH: **Inactivation of akt and NF-kappaB play important roles during indole-3-carbinol-induced apoptosis in breast cancer cells.** *Nutr Cancer* 2004, **48:**84-94.

11. Rahman KW, Sarkar FH: **Inhibition of nuclear translocation of nuclear factor-{kappa}B contributes to 3,3'-diindolylmethane-induced apoptosis in breast cancer cells.** *Cancer Res* 2005, **65:**364-371.

12. Grose KR, Bjeldanes LF: **Oligomerization of indole-3-carbinol in aqueous acid.** *Chem Res Toxicol* 1992, **5:**188-193.

13. Safe S, Papineni S, Chintharlapalli S: **Cancer chemotherapy with indole-3-carbinol, bis(3'-indolyl)methane and synthetic analogs.** *Cancer Lett* 2008, **269:**326-338.

14. Firestone GL, Bjeldanes LF: **Indole-3-carbinol and 3-3'-diindolylmethane antiproliferative signaling pathways control cell-cycle gene transcription in human breast cancer cells by regulating promoter-Sp1 transcription factor interactions.** *J Nutr* 2003, **133:**2448S-2455S.

15. Cover CM, Hsieh SJ, Tran SH, Hallden G, Kim GS, Bjeldanes LF, Firestone GL: **Indole-3-carbinol inhibits the expression of cyclin-dependent kinase-6 and induces a G_1 cell cycle arrest of human breast cancer cells independent of estrogen receptor signaling.** *J Biol Chem* 1998, **273:**3838-3847.

16. Cram EJ, Liu BD, Bjeldanes LF, Firestone GL: **Indole-3-carbinol inhibits CDK6 expression in human MCF-7 breast cancer cells by disrupting Sp1 transcription factor interactions with a composite element in the *CDK6* gene promoter.** *J Biol Chem* 2001, **276:**22332-22340.

17. Jump SM, Kung J, Staub R, Kinseth MA, Cram EJ, Yudina LN, Preobrazhenskaya MN, Bjeldanes LF, Firestone GL: ***N*-Alkoxy derivatization of indole-3-carbinol increases the efficacy of the G_1 cell cycle arrest and of I3C-specific regulation of cell cycle gene transcription and activity in human breast cancer cells.** *Biochem Pharmacol* 2008, **75:**713-724.

18. Nguyen HH, Lavrenov SN, Sundar SN, Nguyen DH, Tseng M, Marconett CN, Kung J, Staub RE, Preobrazhenskaya MN, Bjeldanes LF, Firestone GL: **1-Benzyl-indole-3-carbinol is a novel indole-3-carbinol derivative with significantly enhanced potency of anti-proliferative and anti-estrogenic properties in human breast cancer cells.** *Chem Biol Interact* 2010, **186:**255-266.

19. Kronbak R, Duus F, Vang O: **Effect of 4-methoxyindole-3-carbinol on the proliferation of colon cancer cells in vitro, when treated alone or in combination with indole-3-carbinol.** *J Agric Food Chem* 2010, **58:**8453-8459.

20. Brandi G, Paiardini M, Cervasi B, Fiorucci C, Filippone P, De Marco C, Zaffaroni N, Magnani M: **A new indole-3-carbinol tetrameric derivative inhibits cyclin-dependent kinase 6 expression, and induces G1 cell cycle arrest in both estrogen-dependent and estrogen-independent breast cancer cell lines.** *Cancer Res* 2003, **63:**4028-4036.

21. Lucarini S, De Santi M, Antonietti F, Brandi G, Diamantini G, Fraternale A, Paoletti MF, Tontini A, Magnani M, Duranti A: **Synthesis and biological evaluation of a γ-cyclodextrin-based formulation of the anticancer agent 5,6,11,12,17,18,23,24-octahydrocyclododeca[1,2-*b*:4,5-*b'*:7,8-*b''*:10,11-*b'''*]tetraindole (CTet).** *Molecules* 2010, **15:**4085-4093.

22. Jackson A, Prasitpan N, Shannon P, Tinker A: **Electrophilic substitution in indoles. Part 15. The reaction between methylenedi-indoles and *p*-nitrobenzenediazonium fluoroborate.** *J Chem Soc Perkin Trans 1* 1987, **1:**2543-2551.

23. Amatori S, Bagaloni I, Macedi E, Formica M, Giorgi L, Fusi V, Fanelli M: **Malten, a new synthetic molecule showing *in vitro* antiproliferative activity against tumour cells and induction of complex DNA structural alterations.** *Br J Cancer* 2010, **103:**239-248.

24. **Geospiza.** [http://www.genesifter.net]

25. Cheadle C, Vawter MP, Freed WJ, Becker KG: **Analysis of microarray data using Z score transformation.** *J Mol Diagn* 2003, **5:**73-81.

26. Benjamini Y, Hochberg Y: **Controlling the false discovery rate: a practical and powerful approach to multiple testing.** *J R Statist Soc B* 1995, **57:**289-300.

27. **ArrayExpress.** [http://www.ebi.ac.uk/arrayexpress/].

28. Manning BD, Cantley LC: **AKT/PKB signaling: navigating downstream.** *Cell* 2007, **129:**1261-1274.

29. Seoane J, Le HV, Shen L, Anderson SA, Massagué J: **Integration of Smad and forkhead pathways in the control of neuroepithelial and glioblastoma cell proliferation.** *Cell* 2004, **117:**211-223.

30. Levi F, Bosetti C, Lucchini F, Negri E, La Vecchia C: **Monitoring the decrease in breast cancer mortality in Europe.** *Eur J Cancer Prev* 2005, **14:**497-502.

31. Berry DA, Cronin KA, Plevritis SK, Fryback DG, Clarke L, Zelen M, Mandelblatt JS, Yakovlev AY, Habbema JD, Feuer EJ: **Effect of screening and adjuvant therapy on mortality from breast cancer.** *N Engl J Med* 2005, **353:**1784-1792.

32. Overgaard M, Jensen MB, Overgaard J, Hansen PS, Rose C, Andersson M, Kamby C, Kjaer M, Gadeberg CC, Rasmussen BB, Blichert-Toft M, Mouridsen HT: **Postoperative radiotherapy in high-risk postmenopausal breast-cancer patients given adjuvant tamoxifen: Danish Breast Cancer Cooperative Group DBCG 82c randomised trial.** *Lancet* 1999, **353:**1641-1648.

33. Early Breast Cancer Trialists' Collaborative Group (EBCTCG): **Effects of chemotherapy and hormonal therapy for early breast cancer on recurrence and 15-year survival: an overview of the randomised trials** *Lancet* 2005, **365:**1687-1717.

34. Ferlay J, Autier P, Boniol M, Heanue M, Colombet M, Boyle P: **Estimates of the cancer incidence and mortality in Europe in 2006.** *Ann Oncol* 2007, **18:**581-592.

35. Jemal A, Siegel R, Xu J, Ward E: **Cancer statistics, 2010.** *CA Cancer J Clin* 2010, **60:**277-300.

36. Rahimi M, Huang KL, Tang CK: **3,3'-Diindolylmethane (DIM) inhibits the growth and invasion of drug-resistant human cancer cells expressing EGFR mutants.** *Cancer Lett* 2010, **295:**59-68.

37. Bergman J, Högberg S, Lindström J-O: **Macrocyclic condensation products of indole and simple aldehydes.** *Tetrahedron* 1970, **26:**3347-3352.

38. Staub RE, Bjeldanes LF: **Convenient synthesis of 5,6,11,12,17,18-hexahydrocyclononal[1,2-*b*:4,5-*b'*:7,8-*b''*]triindole, a novel phytoestrogen.** *J Org Chem* 2003, **68:**167-169.

39. Glick D, Barth S, Macleod KF: **Autophagy: cellular and molecular mechanisms.** *J Pathol* 2010, **221:**3-12.

40. White E, DiPaola RS: **The double-edged sword of autophagy modulation in cancer.** *Clin Cancer Res* 2009, **15:**5308-5316.

41. Xiong Y, Hannon GJ, Zhang H, Casso D, Kobayashi R, Beach D: **p21 is a universal inhibitor of cyclin kinases.** *Nature* 1993, **366:**701-704.

42. Wendt J, Radetzki S, von Haefen C, Hemmati PG, Guner D, Schulze-Osthoff K, Dorken B, Daniel PT: **Induction of p21$^{CIP/WAF-1}$ and G2 arrest by ionizing irradiation impedes caspase-3-mediated apoptosis in human carcinoma cells.** *Oncogene* 2006, **25:**972-980.

43. Harper JW, Adami GR, Wei N, Keyomarsi K, Elledge SJ: **The p21 Cdk-interacting protein Cip1 is a potent inhibitor of G1 cyclin-dependent kinases.** *Cell* 1993, **75:**805-816.

44. Harper JW, Elledge SJ, Keyomarsi K, Dynlacht B, Tsai LH, Zhang P, Dobrowolski S, Bai C, Connell-Crowley L, Swindell E, et al.: **Inhibition of cyclin-dependent kinases by p21.** *Mol Biol Cell* 1995, **6:**387-400.

45. Jin S, Antinore MJ, Lung FD, Dong X, Zhao H, Fan F, Colchagie AB, Blanck P, Roller PP, Fornace AJ, Jr., Zhan Q: **The *GADD45* inhibition of Cdc2 kinase correlates with *GADD45*-mediated growth suppression.** *J Biol Chem* 2000, **275:**16602-16608.

46. Gao H, Jin S, Song Y, Fu M, Wang M, Liu Z, Wu M, Zhan Q: **B23 regulates GADD45a nuclear translocation and contributes to GADD45a-induced cell cycle G_2-M arrest.** *J Biol Chem* 2005, **280:**10988-10996.

47. Chai Y, Lee HJ, Shaik AA, Nkhata K, Xing C, Zhang J, Jeong SJ, Kim SH, Lu J: **Penta-O-galloyl-β-D-glucose induces G1 arrest and DNA replicative S-phase arrest independently of P21 cyclin-dependent kinase inhibitor 1A, P27 cyclin-dependent kinase inhibitor 1B and P53 in human breast cancer cells and is orally active against triple-negative xenograft growth.** *Breast Cancer Res* 2010, **12:**R67.

48. Li Y, Upadhyay S, Bhuiyan M, Sarkar FH: **Induction of apoptosis in breast cancer cells MDA-MB-231 by genistein.** *Oncogene* 1999, **18:**3166-3172.

49. Gotea V, Ovcharenko I: **DiRE: identifying distant regulatory elements of co-expressed genes.** *Nucleic Acids Res* 2008, **36:**W133-139.

50. **DIRE (DIstant Regulatory Elements of co-regulated genes.** [http://dire.dcode.org]

51. Zhu QS, Ren W, Korchin B, Lahat G, Dicker A, Lu Y, Mills G, Pollock RE, Lev D: **Soft tissue sarcoma cells are highly sensitive to AKT blockade: a role for p53-independent up-regulation of GADD45α.** *Cancer Res* 2008, **68:**2895-2903.

Figure legends

Figure 1. Synthesis of CTet. Homo-coupling of 2,3'-DIM in presence of formaldehyde in acidic conditions with methanol as a solvent and refluxing the mixture for one hour in the dark.

Figure 2. Antiproliferative activity of the CTet formulated in γ-cyclodextrin aqueous solution. Estrogen receptor positive (MCF-7 and BT-474) and triple-negative (MDA-MB-231 and BT-20) human breast cancer cell lines were exposed to increased concentrations of CTet. Cell proliferation was evaluated by [^{3}H]thymidine incorporation into cellular DNA after 72 hours of treatment. Results are shown as the percentage of [^{3}H]thymidine incorporation in treated cells compared with control cells (vehicle only). Data are expressed as mean ± SEM of at least three separate experiments.

Figure 3. Cell cycle effects of the CTet in MCF-7 and MDA-MB-231 cell lines. DNA content profiles obtained from cells exposed for 24 and 48 hours to 4 μM and 8 μM of CTet or γ-cyclodextrin solution (CTR), stained with propidium iodide and analyzed by flow cytometry. Figures are from one representative experiment; The percentages of cell number in the different phases of cell cycle are represented as means of three experiments ± SEM. Asterisks indicate

statistically significant values respect to CTR; one-way ANOVA followed by Tukey post-hoc test ($p<0.05$).

Figure 4. Morphological features of autophagy in CTet-treated MDA-MB-231 cells. Autophagy induction in MDA-MB-231 cells following exposure to CTet was detected by recruitment of LC3b protein to autophagosomes (A) and fusion between autophagosomes and lysosomes, in terms of co-localization of LC3b and the lysosome marker LAMP2a (B).

Figure 5. Gene expression analysis of p27, p21 and GADD45A. Quantitative real-time PCR (grey bars) and microarray-based (black bars) expression analyses of p27, p21 and GADD45A genes were carried out in MCF-7 and MDA-MB-231 cell lines treated with CTet 6.0 μM (left) and 12.0 μM (right) for 24 hours. For quantitative real-time PCR, GAPDH was used as housekeeping gene. Data are shown as mean ± standard deviation. Asterisks indicate statistically significant values ($p<0.01$).

Figure 6. Cell viability and immunoblot analyses in CTet-treated MCF-7 and MDA-MB-231 breast cancer cell lines. Cells were treated for 24 and 48 hours with 6.0 and 12.0 μM CTet or vehicle only (γ-cyclodextrin aqueous solution); after treatments, cell viability was evaluated by Trypan blue dye exclusion assay and cell extracts were processed as described in methods for immunoblot analyses. Akt activity was analyzed using a phospho-sensitive Akt antibody in total cell extracts and in cytosolic cellular fractions; FOXO3a localization was evaluated by separation of nuclear and cytosolic proteins; p21 and p27 overexpression were evaluated in total cell extracts. FOXO3a, p27 and p21 were normalized to actin; phospho-Akt were normalized to total-Akt. Cell counts are the means ± SEM of three separate experiments. Asterisks indicate statistically significant values respect to untreated cells; one-way ANOVA followed by Tukey post-hoc test ($p<0.01$). Blots are representative of at least two separate experiments.

Figure 7. *In vivo* effects of CTet on the growth of human MCF-7 breast cancer cells-derived tumors from xenografts in athymic mice. Athymic female mice were inoculated with MCF-7 cells and then intraperitoneally treated with CTet (5 mg/Kg) or vehicle (γ-cyclodextrin solution) for 2 weeks as described under materials and methods section. The percentage of residual tumor mass has been calculated respect to time 0 corresponding to the start of treatment. Positive control (CTR): 4 mice bearing the tumor and not treated; CTR + vehicle: 4 mice bearing the tumor receiving the vehicle; CTR + CTet: 5 mice bearing the tumor receiving CTet. The results are mean ± S.D. of the number of mice indicated above. Asterisk: statistically significant value respect to CTR and CTR+vehicle; Mann-Whitney test, $p<0.05$.

Table 1: Selected ontologies of commonly up-regulated genes. Sub-categories within a given ontology are shown in italics

Term	Genes*	Gene Set on the array	z-score
Biological process			
response to stimulus	39	3137	4.82
response to stress	27	1753	5.05
response to unfolded protein	3	62	4.14
acute inflammatory response	5	99	5.5
acute-phase response	4	43	7.11
regulation of acute inflammatory response	3	26	6.95
response to chemical stimulus	21	1396	4.26
response to organic substance	15	845	4.25
response to hormone stimulus	10	440	4.35
response to steroid hormone stimulus	7	220	4.75
response to glucocorticoid stimulus	6	94	6.98
leukocyte chemotaxis	3	60	4.23
response to oxygen levels	5	151	4.12
response to toxin	3	64	4.05
response to extracellular stimulus	7	242	4.41
positive regulation of response to external stimulus	4	87	4.63
cellular response to extracellular stimulus	5	82	6.19
cellular response to nutrient levels	4	62	5.73
cellular response to starvation	3	43	5.2
response to biotic stimulus	10	424	4.49
response to virus	6	147	5.24
cell death	24	1227	6.04
apoptosis	22	1116	5.8
regulation of cell death	17	872	4.99
regulation of apoptosis	16	859	4.62

negative regulation of cell death	10	402	4.69
negative regulation of apoptosis	9	391	4.16
induction of apoptosis	8	333	4.06
anti-apoptosis	8	226	5.49
positive regulation of anti-apoptosis	3	32	6.18
cellular component disassembly involved in apoptosis	3	27	6.81
release of cytochrome c from mitochondria	3	24	7.27
protein folding	6	158	4.99
leukocyte migration	4	86	4.66
autophagy	3	48	4.86
regulation of synaptic plasticity	3	57	4.37
iron ion homeostasis	4	31	8.54
positive regulation of smooth muscle cell proliferation	3	28	6.67
regulation of viral reproduction	3	28	6.67
Cellular component			
integral to membrane	9	4459	-4.27
autophagic vacuole	3	20	8.2
Molecular functions			
heat shock protein binding	5	71	7.14
unfolded protein binding	5	103	5.69
antioxidant activity	3	45	5.35

* number of genes differentially expressed within the assigned ontology.

Table 2: Selected ontologies of commonly down-regulated genes. Sub-categories within a given ontology are shown in italics

Term	Genes*	Gene Set on the array	z-score
Biological process			
cell cycle	20	957	4.42
spindle organization	4	54	5.31
DNA metabolic process	18	559	6.32
DNA replication	13	228	8.13
DNA-dependent DNA replication	5	71	5.75
DNA-dependent DNA replication initiation	3	25	6.13
Cellular component			
chromosomal part	13	381	5.57
condensed chromosome kinetochore	4	69	4.52
replication fork	3	33	5.2
Molecular function			
transmembrane receptor protein tyrosine kinase activity	4	64	4.81
DNA helicase activity	3	41	4.6
insulin-like growth factor binding	3	24	6.32

* number of genes differentially expressed within the assigned ontology.

Additional data files

Additional data file 1. CTr formation. Plausible mechanisms of CTr formation in the CTet synthesis.

Format: .PDF

Additional data file 2. Figure 1S Autophagic morphological features induced by serum starvation in MDA-MB-231 cells (positive control) detected by fusion between autophagosomes and lysosomes, in terms of co-localization of LC3b and the lysosome marker LAMP2a.

Format: .PDF

Additional data file 3. Table 1S Transcriptome analysis was performed on MCF-7 and MDA-MB-231 cells treated with 6.0 μM and 12.0 μM CTet for 24 hours. The genes up-regulated in both MCF-7 and MDA-MB-231 cell lines, either in 6.0 μM and 12.0 μM CTet treatment conditions, were selected using GeneSifter software. The software analysis allowed to identify a list of 116 genes significantly (p<0.01) up-regulated in both cell lines.

Format: .PDF

Additional data file 4. Table 2S Transcriptome analysis was performed on MCF-7 and MDA-MB-231 cells treated with 6.0 μM and 12.0 μM CTet for 24 hours. The genes down-regulated in both MCF-7 and MDA-MB-231 cell lines, either in 6.0 μM and 12.0 μM CTet treatment conditions, were selected using GeneSifter software. The software analysis allowed to identify a list of 177 genes significantly (p<0.01) down-regulated in both cell lines.

Format: .PDF

Additional data file 5. Fig. 2S Quantitative real-time PCR of p27, p21 and GADD45A genes were carried out in MCF-7 and MDA-MB-231 cell lines treated with CTet 6.0 μM (left) and 12.0 μM (right) for 24 hours. Data are shown as mean ± standard deviation of three separate experiments. Asterisks indicate statistically significant values ($p<0.01$).

Format: .PDF

Additional data file 6. Table 3S Antiproliferative activity of CTet in different storing conditions in MCF-7 cells. Aliquots of CTet were stored at different conditions of temperature and light exposition and the activity was then evaluated in MCF-7 at different time points (4, 8, 12, 20 weeks and after one year). Results are reported as IC_{50} values.

Format: .PDF

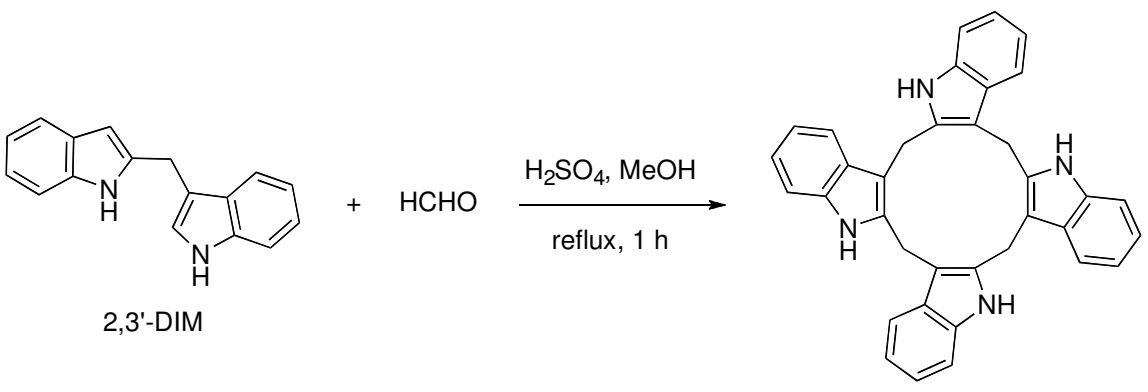

Figure 1

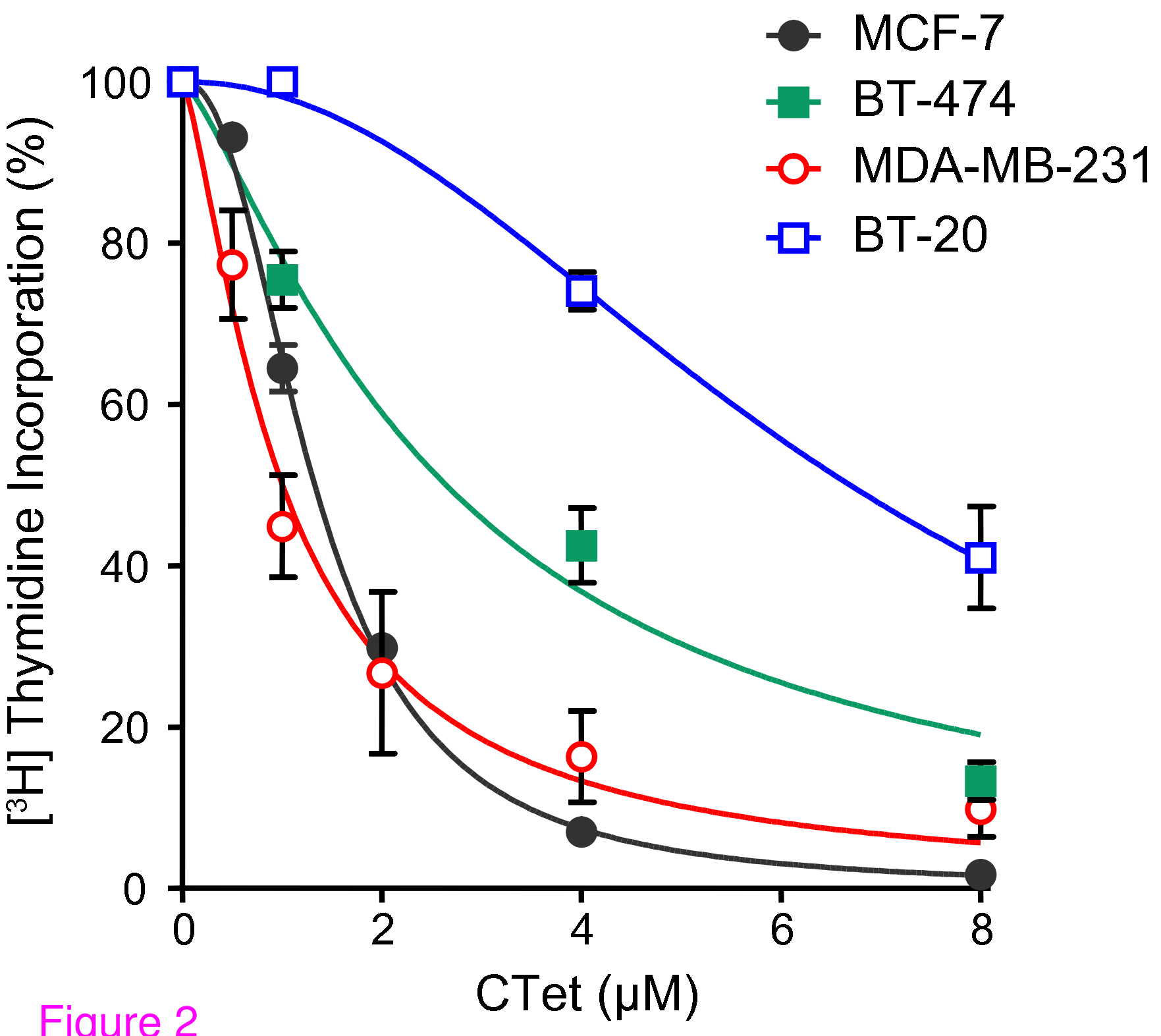
MCF-7
BT-474
MDA-MB-231
BT-20
[3H] Thymidine Incorporation (%)
100
80
60
40
20
0
0
2
4
6
8
CTet (μM)

Figure 2

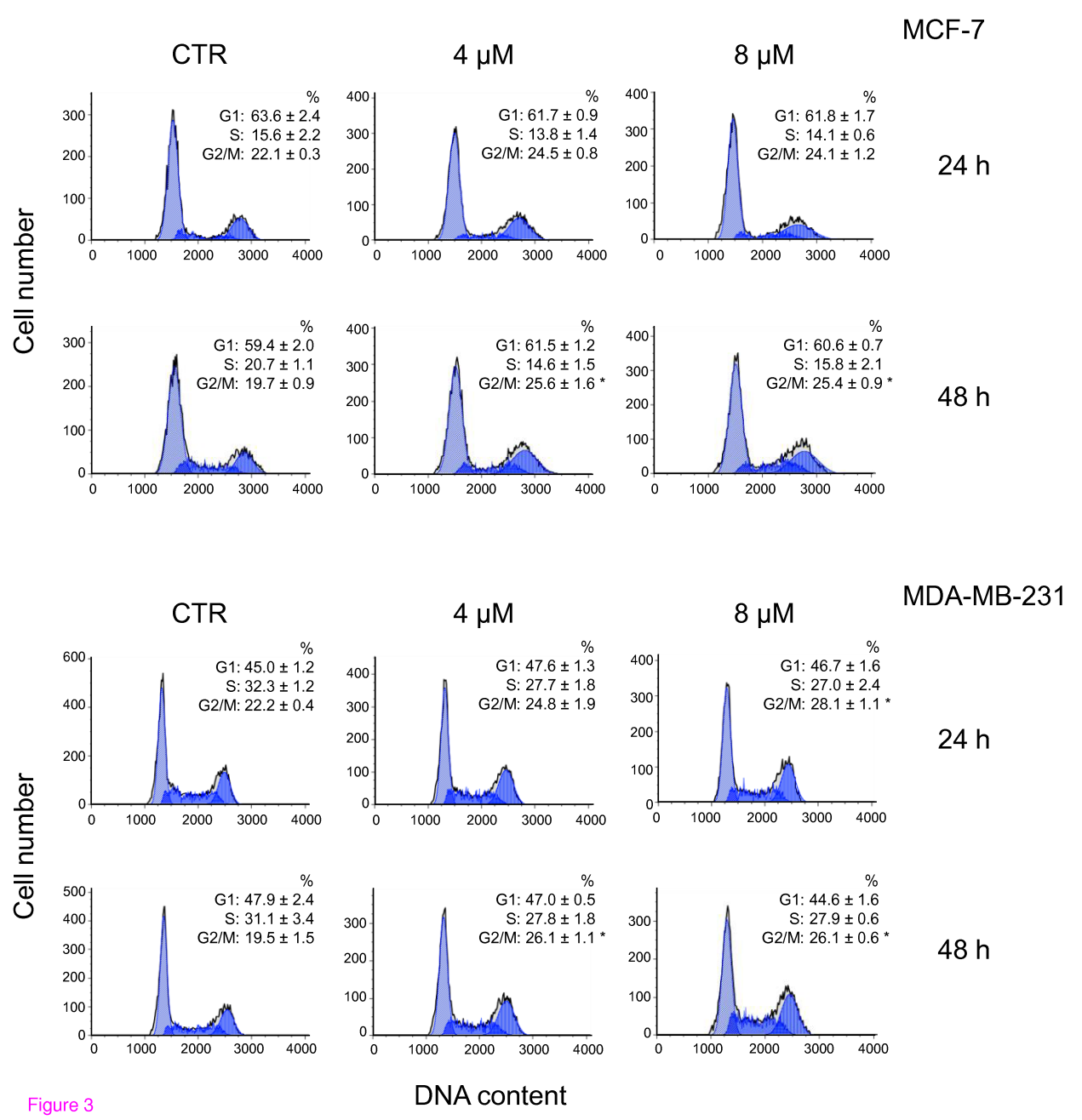
MCF-7
CTR
4 μM
8 μM
24 h
48 h
%
G1: 63.6 ± 2.4
S: 15.6 ± 2.2
G2/M: 22.1 ± 0.3
G1: 61.7 ± 0.9
S: 13.8 ± 1.4
G2/M: 24.5 ± 0.8
G1: 61.8 ± 1.7
S: 14.1 ± 0.6
G2/M: 24.1 ± 1.2
G1: 59.4 ± 2.0
S: 20.7 ± 1.1
G2/M: 19.7 ± 0.9
G1: 61.5 ± 1.2
S: 14.6 ± 1.5
G2/M: 25.6 ± 1.6 *
G1: 60.6 ± 0.7
S: 15.8 ± 2.1
G2/M: 25.4 ± 0.9 *
MDA-MB-231
G1: 45.0 ± 1.2
S: 32.3 ± 1.2
G2/M: 22.2 ± 0.4
G1: 47.6 ± 1.3
S: 27.7 ± 1.8
G2/M: 24.8 ± 1.9
G1: 46.7 ± 1.6
S: 27.0 ± 2.4
G2/M: 28.1 ± 1.1 *
G1: 47.9 ± 2.4
S: 31.1 ± 3.4
G2/M: 19.5 ± 1.5
G1: 47.0 ± 0.5
S: 27.8 ± 1.8
G2/M: 26.1 ± 1.1 *
G1: 44.6 ± 1.6
S: 27.9 ± 0.6
G2/M: 26.1 ± 0.6 *
Cell number
DNA content

Figure 3

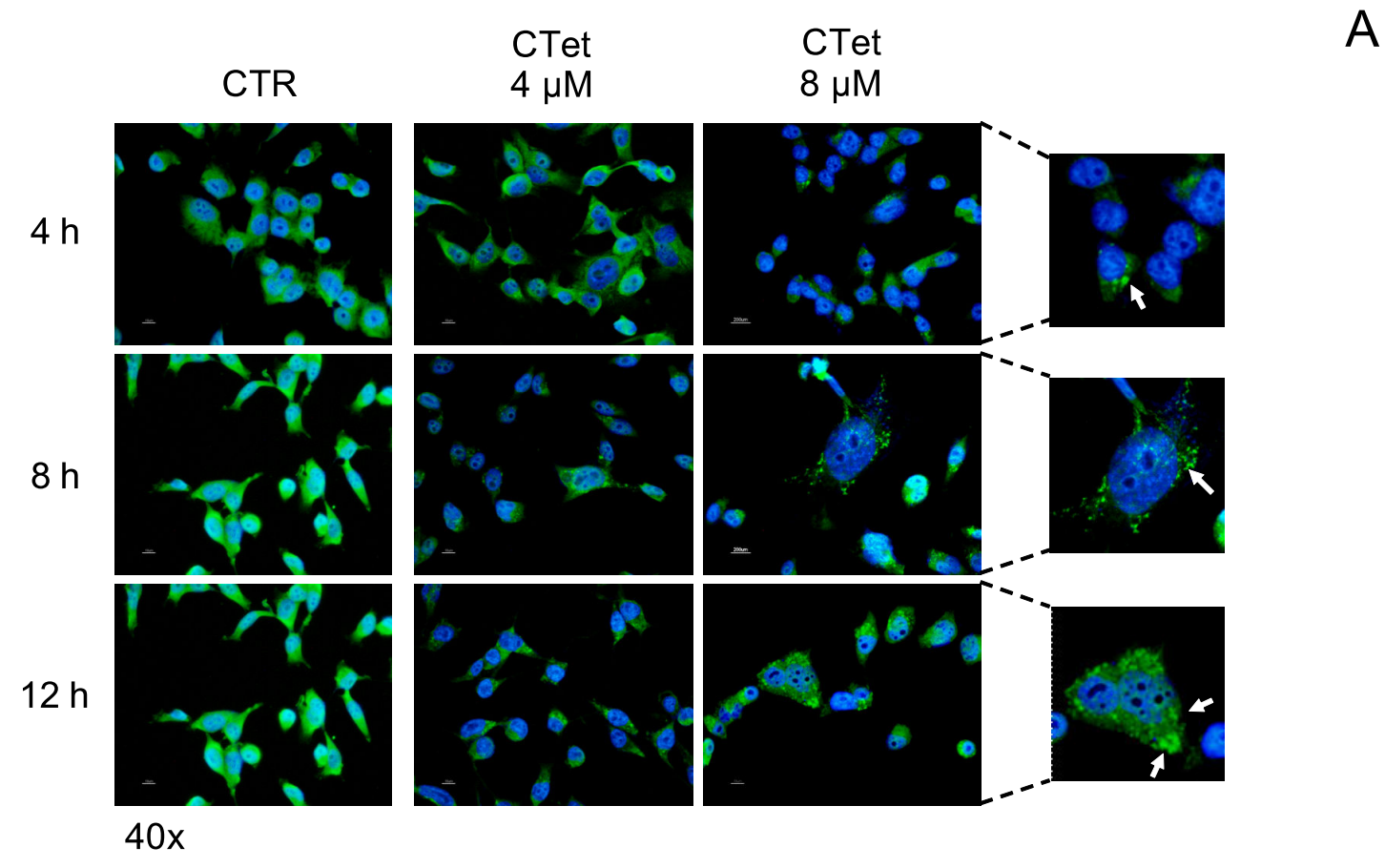
A
CTR
CTet
4 µM
CTet
8 µM
4 h
8 h
12 h
40x

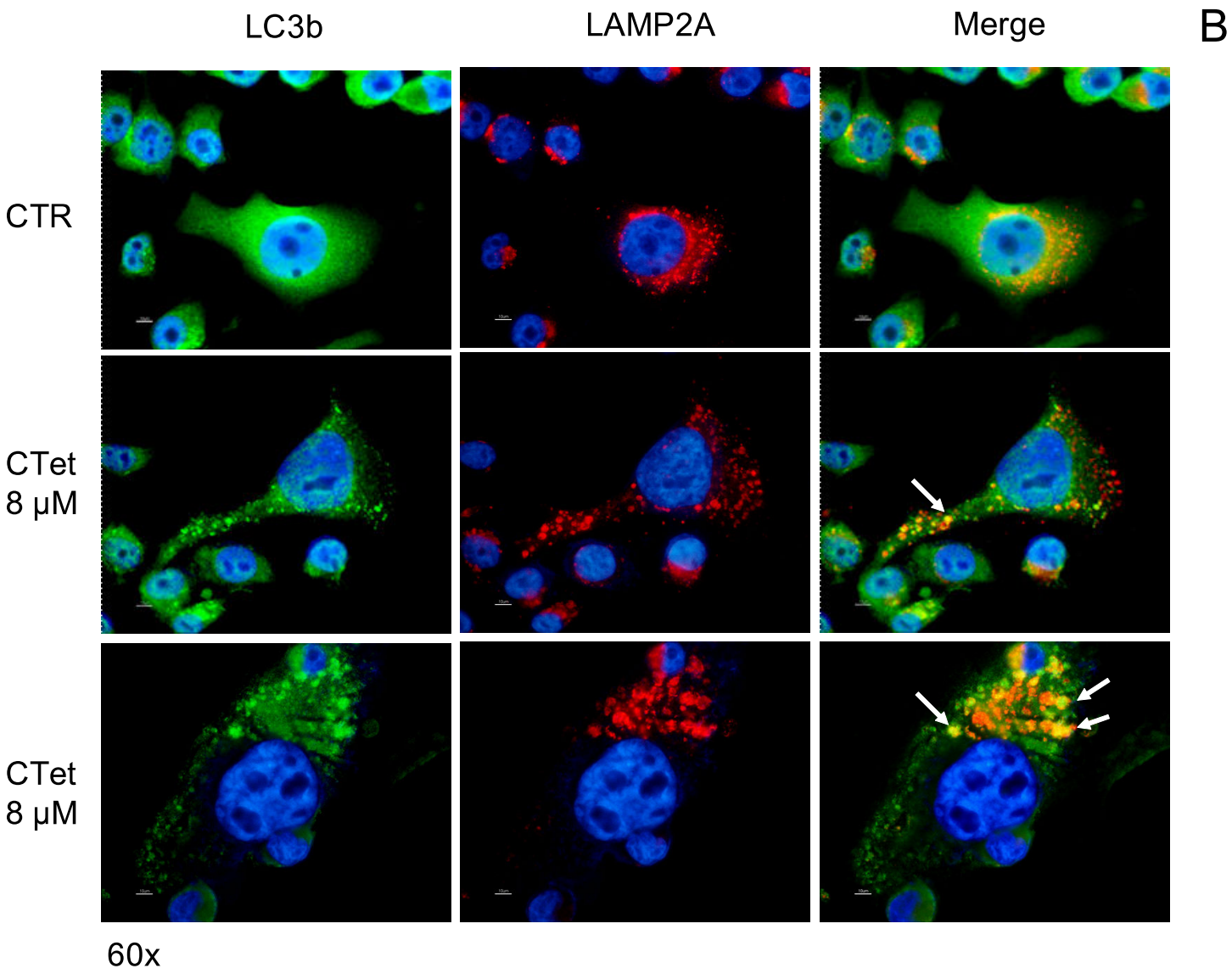
B
LC3b
LAMP2A
Merge
CTR
CTet
8 µM
CTet
8 µM
60x

Figure 4

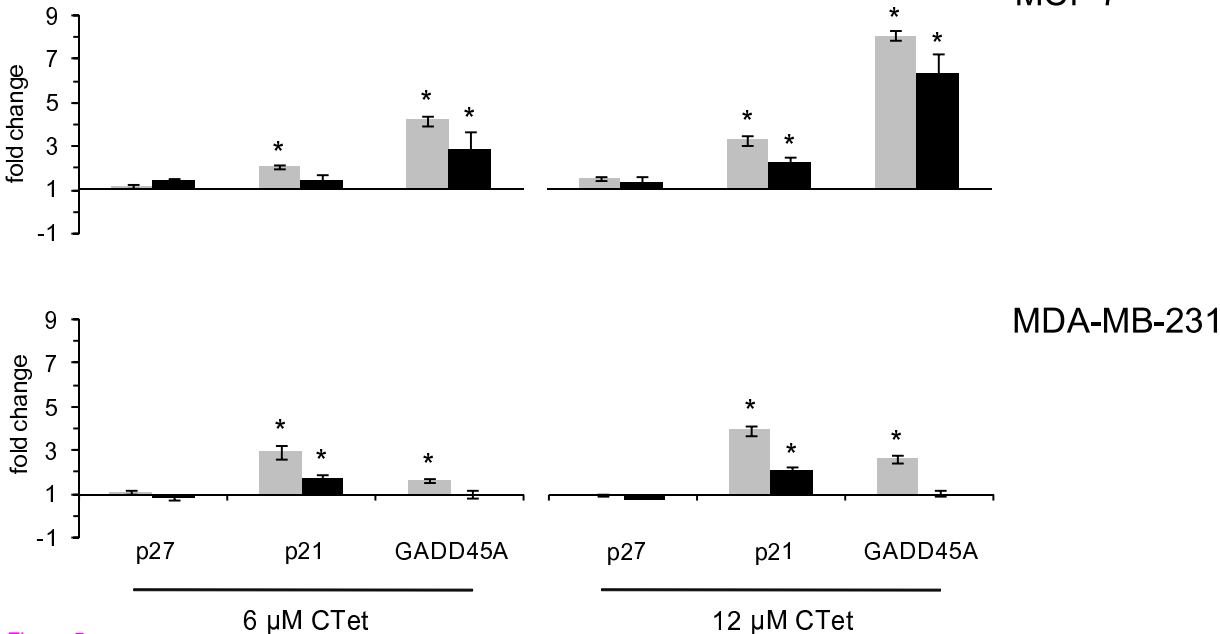
MCF-7
MDA-MB-231
fold change
9
7
5
3
1
-1
*
p27
p21
GADD45A
6 μM CTet
12 μM CTet

Figure 5

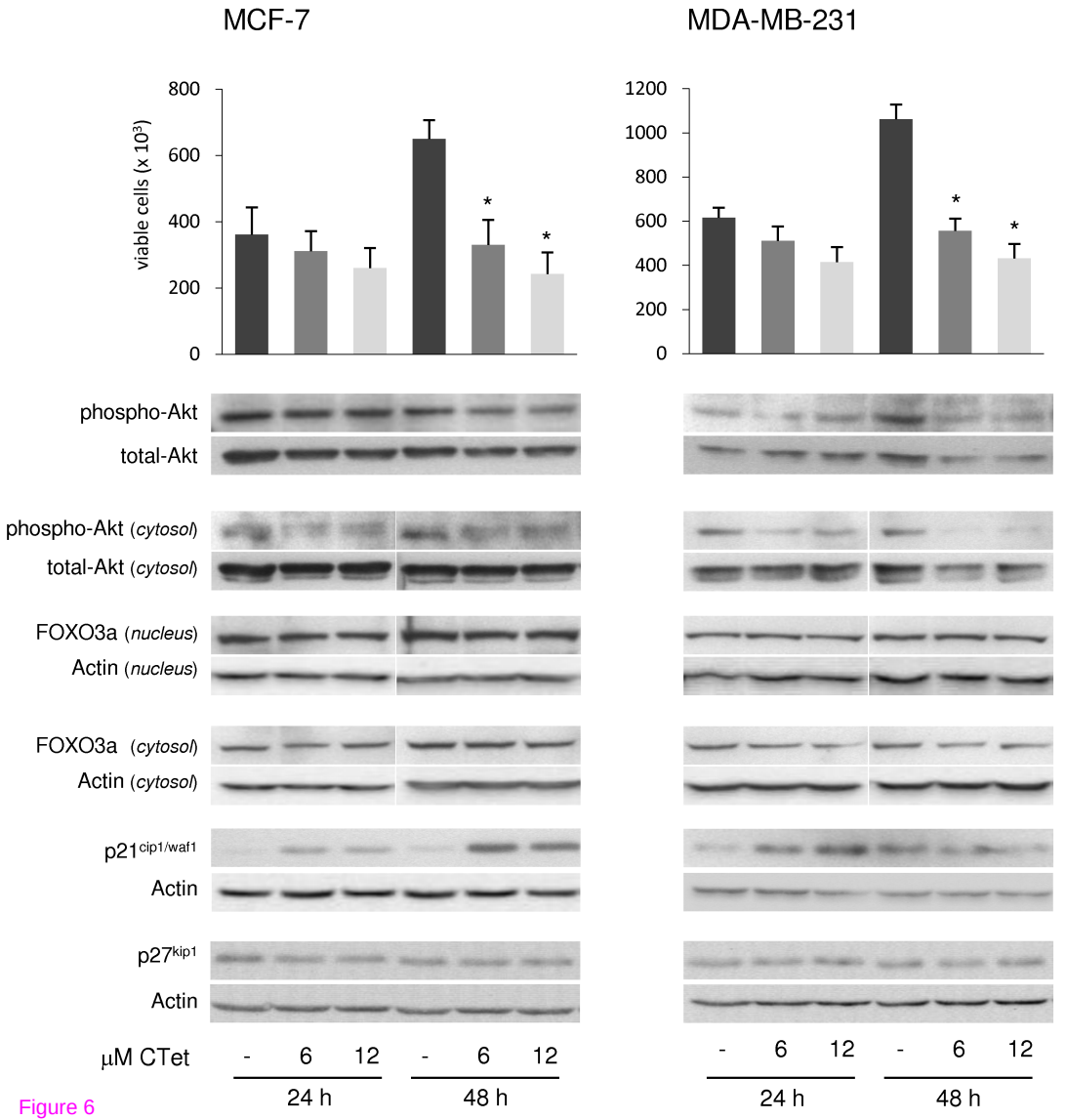
MCF-7
MDA-MB-231
viable cells (x 10³)
800
600
400
200
0
1200
1000
800
600
400
200
0
*
*
*
*
phospho-Akt
total-Akt
phospho-Akt (cytosol)
total-Akt (cytosol)
FOXO3a (nucleus)
Actin (nucleus)
FOXO3a (cytosol)
Actin (cytosol)
p21cip1/waf1
Actin
p27kip1
Actin
μM CTet
- 6 12 - 6 12
- 6 12 - 6 12
24 h
48 h
24 h
48 h

Figure 6

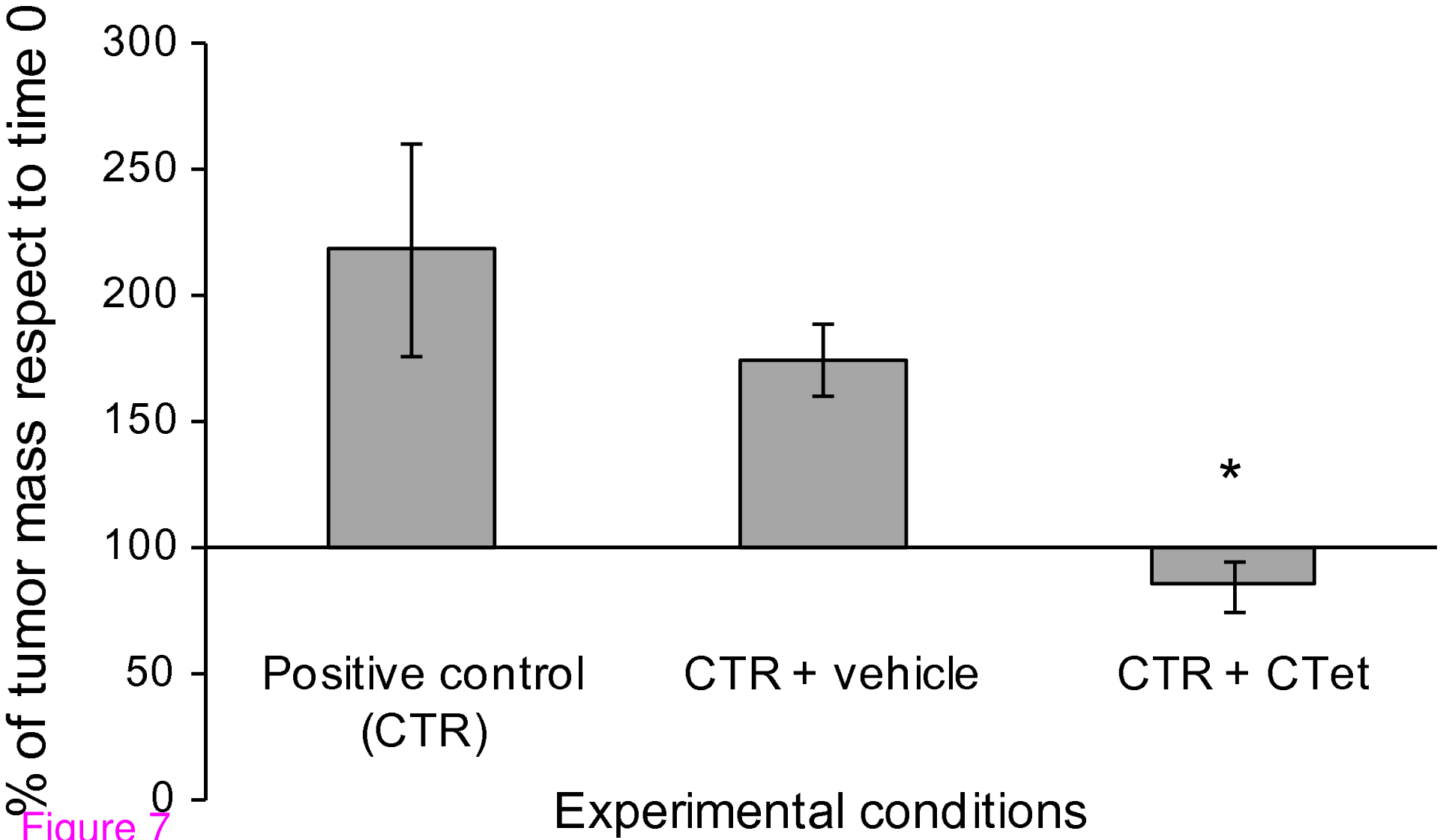
% of tumor mass respect to time 0
300
250
200
150
100
50
0
*
Positive control (CTR)
CTR + vehicle
CTR + CTet
Experimental conditions

Figure 7

Additional files provided with this submission:

Additional file 1: Additional Data File 1 - CTr formation.pdf.pdf, 52K
http://breast-cancer-research.com/imedia/1199338166528492/supp1.pdf
Additional file 2: Additional Data File 2 - Fig. 1S.pdf.pdf, 69K
http://breast-cancer-research.com/imedia/2985979595284927/supp2.pdf
Additional file 3: Additional Data File 3 - Table 1S.pdf.pdf, 65K
http://breast-cancer-research.com/imedia/1448752889528492/supp3.pdf
Additional file 4: Additional Data File 4 - Table 2S.pdf.pdf, 91K
http://breast-cancer-research.com/imedia/1412836245528492/supp4.pdf
Additional file 5: Additional Data File 5 - Fig. 2S.pdf.pdf, 503K
http://breast-cancer-research.com/imedia/2496132645284927/supp5.pdf
Additional file 6: Additional Data File 6 - Table 3S.pdf.pdf, 75K
http://breast-cancer-research.com/imedia/6130228185284927/supp6.pdf